

THE INVERSE CASCADE IN TURBULENT DYNAMOS

AXEL BRANDENBURG

*Nordita, Blegdamsvej 17, DK-2100 Copenhagen Ø, Denmark
 Mathematics Department, Univ. of Newcastle, NE1 7RU, UK*

Abstract. The emergence of a large scale magnetic field from randomly forced isotropic strongly helical flows is discussed in terms of the inverse cascade of magnetic helicity and the α -effect. In simulations of such flows the maximum field strength exceeds the equipartition field strength for large scale separation. However, helicity conservation controls the speed at which this final state is reached. In the presence of open boundaries magnetic helicity fluxes out of the domain are possible. This reduces the timescales of the field growth, but it also tends to reduce the maximum attainable field strength.

1. Introduction

It was since the mid-seventies when Frisch *et al.* (1975) and Pouquet *et al.* (1976) came up with the idea that the large scale magnetic fields seen in many astrophysical bodies could be caused by an inverse cascade-type phenomenon. Although there were close links with earlier results that helicity and lack of mirror symmetry are important (Steenbeck *et al.* 1966; see also Krause & Rädler 1980), the notion of an inverse cascade has put dynamo theory into a self-consistent framework of nonlinear turbulence theory.

Unfortunately the inverse cascade concept was not easily assimilated by the astrophysical community. The reasons are simple: the inverse cascade approach was developed in the framework of isotropic homogeneous turbulence, and was not readily applicable to astrophysical bodies that were stratified and enclosed in boundaries. Thus, people continued to use α^2 and $\alpha\Omega$ -dynamos (Moffatt 1978), which enabled modelling of a large variety of astrophysical bodies.

Here we want is to look more closely at inverse cascade dynamos. In particular, we want to know what kind of field they produce and how this

relates to the fields generated by an α^2 -dynamo. The full results of this work are presented in a separate paper (Brandenburg 2000, hereafter referred to as B2000). In the present paper we also discuss the effects of open boundaries allowing magnetic helicity fluxes out of the domain into the exterior or across the equator. This is an important issue that has been raised recently in the context of dynamo theory (Blackman & Field 2000, Kleeorin *et al.* 2000).

In order to model isotropic random flows we adopt a forcing function that consists of randomly oriented Beltrami fields with a wavenumber, k_f , that is larger than the smallest wavenumber, k_1 , that fits into the box. For most of the calculations we use $k_f = 5$ and $k_1 = 1$, leaving some margin for scale separation. In order to see more clearly the effects of scale separation we also have one run where $k_f = 30$. In the wavenumber band $4.5 < |\mathbf{k}| < 5.5$ (for $k_f = 5$) there are 350 wavevectors which are chosen randomly at each timestep, so the forcing is δ -correlated in time, but the resulting velocity field is not. In fact, the velocity has a well defined correlation time that agrees well with the turnover time $\tau = \ell_f/u_{\text{rms}}$, where $\ell_f = 2\pi/k_f$ is the forcing scale and u_{rms} is the rms velocity.

The degree of turbulence that develops depends on the range of length scales left between the forcing scale and the dissipative cutoff scale. A reasonable range can only be obtained if the forcing wavenumber is not too high, so the run with $k_f = 30$ (Run 6 in B2000) is an example where the flow is laminar on the forcing scale. The degree of mixing, as measured by the ratio of the turbulent to the microscopic diffusion coefficients for a passive scalar, D_t/D , is here of order one. In a more turbulent run, Run 3 of B2000, this ratio is around 40. However, quite independently of how turbulent a run is, we find the emergence of a large scale magnetic field after some time. The resulting field resembles closely that obtained from an α^2 -dynamo with the same (periodic) boundary conditions. This analogy enables us to make contact with mean-field theory and to explain the resulting turbulent transport coefficients.

2. Emergence of a large scale field

The inverse cascade is traditionally described in terms of energy spectra. In Figure 1 we compare the spectral field evolution for two different forcing wavenumbers. Note that the envelope of the magnetic energy fits underneath a k^{-1} slope. The peaks at $k = k_1$ and k_f also fit underneath the same slope. There are several features of the spectrum that are characteristic also of other cases investigated. For large enough scale separation one sees that the magnetic energy grows fast at two distinct wavenumbers, $k \approx 30$ and $k \approx 7$. However, when the energy at $k \sim 7$ reaches saturation the energy

begins to be transferred to larger scales until much of the magnetic energy is at the largest scale possible. During this phase the magnetic energy at intermediate scales decreases to some minimum value which follows roughly a $k^{+3/2}$ spectrum. This effect may be referred to as ‘self-cleaning’, because by removing energy at intermediate scales the field at the largest scales appears less perturbed and hence cleaner. This self-cleaning effect is the result of nonlinearity, which suppresses the growth at intermediate scales. However, the type of nonlinearity does not seem to matter: even with ambipolar diffusion the same behaviour is found (Brandenburg & Subramanian 2000).

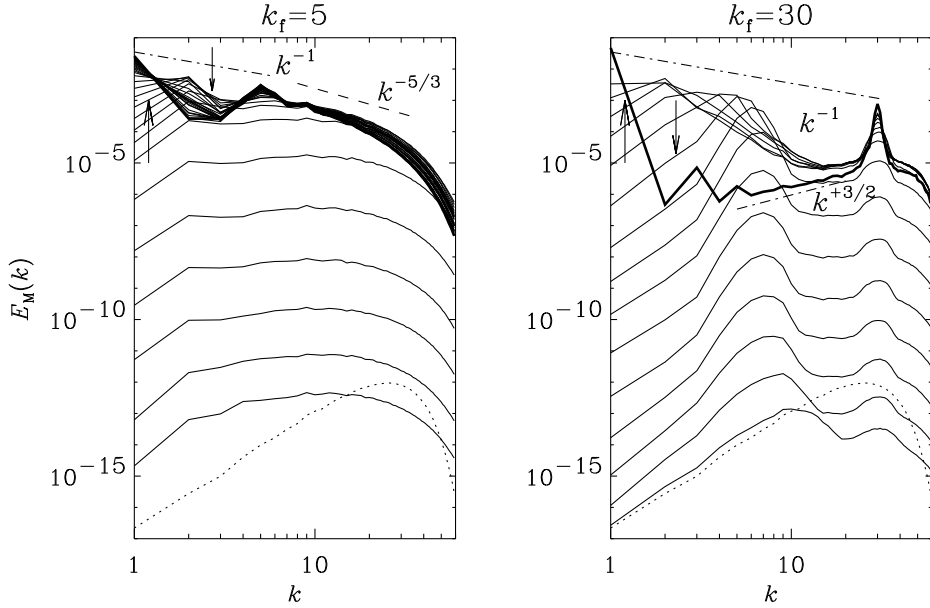


Figure 1. Magnetic energy spectra for runs with small and large scale separation, $k_f = 5$ and 30, respectively.

In Figure 2 we show cross-sections of B_x at different times. Towards the end of the evolution the large scale magnetic field is essentially a Beltrami field which is here of the form $\bar{\mathbf{B}} \sim (\sin y, 0, \cos y)$, apart from some phase shift in y .

3. The final equilibrium field strength

Characteristic to all the runs reported in B2000 is the fact that super-equipartition field strengths are reached. In Figure 3 the evolution of magnetic and kinetic energies are shown for two runs with different forcing wavenumbers. Note also the extremely slow evolution past the moment

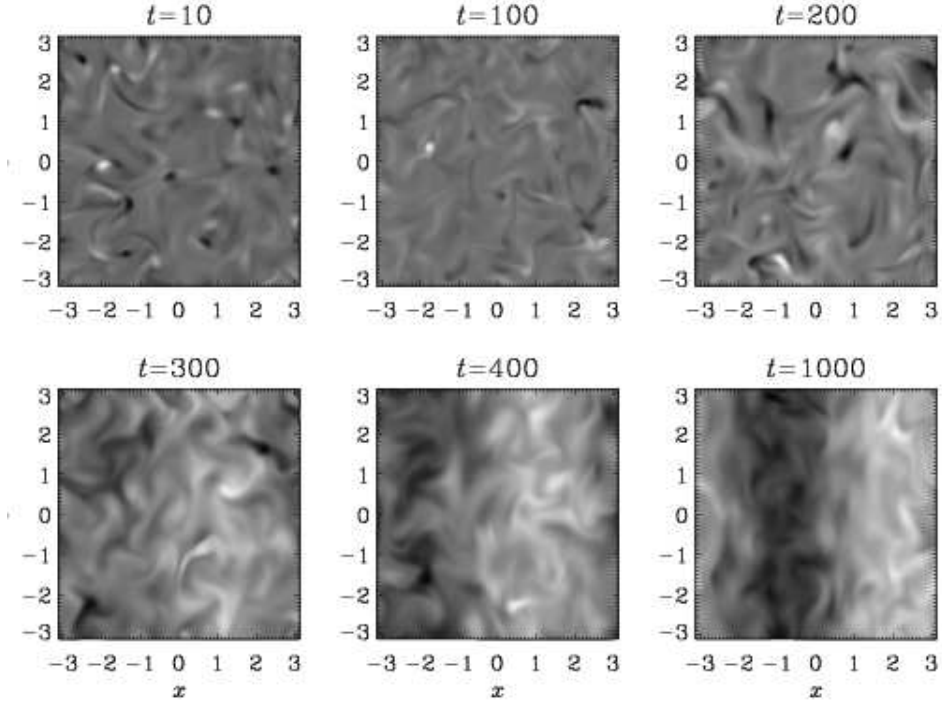


Figure 2. Gray-scale images of cross-sections of $B_x(x, y, 0)$ for Run 3 of B2000 at different times showing the gradual build-up of the large scale magnetic field after $t = 300$. Dark (light) corresponds to negative (positive) values. Each image is scaled with respect to its min and max values.

where the kinetic energy drops suddenly to a smaller value. This is when saturation of small scale magnetic energy is reached. However, after that moment the large scale magnetic energy continues to grow for some time, because the resulting large scale field is force-free and does hence not affect the velocity field directly.

The prolonged saturation behaviour found in the present simulations is at first glance unusual. Since at late times most of the magnetic energy is in the large scales, this slow evolution must have to do with the properties of the large scale field. An important property of this large scale field is that it possesses magnetic helicity. At the same time magnetic helicity is conserved by the nonlinear terms and can hence only change resistively on an ohmic timescale. (The case with open boundaries is different and will be discussed separately.) In order to demonstrate magnetic helicity conservation we consider a periodic box and write the magnetic field, \mathbf{B} , as the curl of a vector potential, \mathbf{A} , so $\mathbf{B} = \nabla \cdot \mathbf{A}$. We use the uncurled

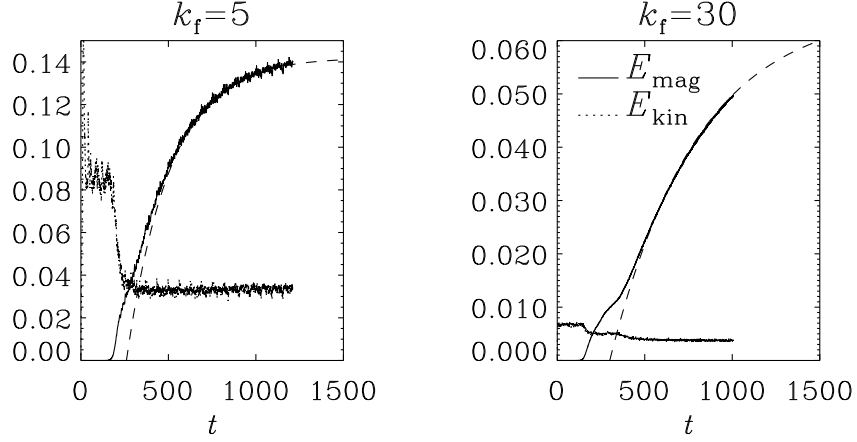


Figure 3. Evolution of kinetic (dotted) and magnetic (solid) energies. The slow evolution of the magnetic energy follows approximately the $1 - e^{-2\eta\Delta t}$ behaviour (dashed line) of Eq. (6) that results from helicity conservation.

induction equation,

$$\partial \mathbf{A} / \partial t = \mathbf{u} \times \mathbf{B} - \eta \mathbf{J} - \nabla \phi, \quad (1)$$

where $\mathbf{J} = \nabla \times \mathbf{B}$ is the current density, η is the magnetic diffusivity, and ϕ is the electrostatic potential. The magnetic helicity, which can be defined as $\langle \mathbf{A} \cdot \mathbf{B} \rangle$, satisfies

$$d\langle \mathbf{A} \cdot \mathbf{B} \rangle / dt = -2\eta \langle \mathbf{J} \cdot \mathbf{B} \rangle, \quad (2)$$

where angular brackets denote volume averages over the periodic domain. The steady state solution must satisfy $\langle \mathbf{J} \cdot \mathbf{B} \rangle = 0$, so small and large scale current helicities must be comparable in magnitude, $|\langle \mathbf{j} \cdot \mathbf{b} \rangle| \approx |\langle \overline{\mathbf{J}} \cdot \overline{\mathbf{B}} \rangle|$, but of opposite sign. The magnetic helicity is however concentrated on large scales (its spectrum is k^2 times that of the current helicity), so its small scale contribution is negligible.

We measure the degree of magnetic helicity of the large scale field by the quantity $k_{AB}^{-1} = |\langle \overline{\mathbf{A}} \cdot \overline{\mathbf{B}} \rangle| / \langle \overline{\mathbf{B}}^2 \rangle$, which is a length scale characterizing the scale of the helical contribution. In a periodic domain of size L the smallest wavenumber is $k_1 = 2\pi/L$, and so k_{AB} is bounded from above by $k_{AB} \leq k_1$. The large scale current helicity is k_1^2 times the magnetic helicity, so we have

$$\langle \overline{\mathbf{A}} \cdot \overline{\mathbf{B}} \rangle = \mp \langle \overline{\mathbf{B}}^2 \rangle / k_{AB} = \langle \overline{\mathbf{J}} \cdot \overline{\mathbf{B}} \rangle / k_1^2, \quad (3)$$

where the upper sign applies to the case of positive kinetic helicity in the turbulence. Using this in Eq. (2) together with $\langle \mathbf{A} \cdot \mathbf{B} \rangle \approx \langle \overline{\mathbf{A}} \cdot \overline{\mathbf{B}} \rangle$ and

$\langle \mathbf{J} \cdot \mathbf{B} \rangle = \langle \overline{\mathbf{J}} \cdot \overline{\mathbf{B}} \rangle + \langle \mathbf{j} \cdot \mathbf{b} \rangle$ yields

$$\mp d\langle \overline{\mathbf{B}}^2 \rangle / dt = \pm 2\eta k_1^2 \langle \overline{\mathbf{B}}^2 \rangle - 2\eta k_{AB} \langle \mathbf{j} \cdot \mathbf{b} \rangle. \quad (4)$$

Prior to saturation $\langle \mathbf{j} \cdot \mathbf{b} \rangle$ is small, but during saturation its value is limited by the kinetic helicity, so

$$\langle \mathbf{j} \cdot \mathbf{b} \rangle \approx \langle \rho \rangle \langle \boldsymbol{\omega} \cdot \mathbf{u} \rangle \approx \pm k_f \langle \rho \mathbf{u}^2 \rangle = \pm k_f B_{\text{eq}}^2 / \mu_0. \quad (5)$$

This yields an evolution equation for the mean magnetic field,

$$\frac{\langle \overline{\mathbf{B}}^2 \rangle}{B_{\text{eq}}^2} \approx \frac{k_f k_{AB}}{k_1^2} \left\{ 1 - \exp \left[-2\eta k_1^2 (t - t_{\text{sat}}) \right] \right\}, \quad (6)$$

which is only valid at late times when $\Delta t \equiv t - t_{\text{sat}} > 0$. (Here, t_{sat} is the time when the small scale field saturates.) We emphasize that this relation is rather general and independent of the actual model of field amplification, because we used only the concept of magnetic helicity conservation. The important point here is that full saturation is only obtained after an ohmic diffusion time. In that sense Eq. (6) poses a constraint on the mean magnetic field at late times. It applies only as long as the magnetic field is helical. Indeed, lower degrees of helicity, i.e. smaller values of k_{AB}^{-1} , allow larger values of the final field strength; see Eq. (6). This has been verified in a model where differential rotation or shear contributed significantly to the field amplification (Brandenburg *et al.* 2000). However, this only relaxes the constraint by a certain factor which depends on the degree of helicity of the large scale field which, in turn, depends on the degree of linkage of poloidal and toroidal field. We found that to a good approximation this factor is given by the ratio Q of toroidal to poloidal field strengths. In the sun this factor is less than a hundred, so this is a relatively minor effect compared with the value of the magnetic Reynolds number ($10^8 - 10^{10}$).

4. Helicity exchange across the equator

A different way of relaxing the slow growth problem is to allow for fluxes out of the dynamo volume either into the exterior of the dynamo (the corona or halo) or from one hemisphere to the other. In any case, there would be an extra surface term in Eq. (2). Here we want to discuss the latter alternative of a helicity flux between the two hemispheres. Such a flux could result from a turbulent exchange of magnetic helicity between the two hemispheres and should therefore be proportional to some turbulent magnetic diffusivity η_t . Based on dimensional arguments, one may expect such a term to be of the form $\eta_t k_{\text{eff}}^2 H$, where H is the gauge-invariant

magnetic helicity for open volumes (Berger & Field 1984), which replaces $\langle \mathbf{A} \cdot \mathbf{B} \rangle$. The diffusion of magnetic helicity depends on the length scale $2\pi/k_{\text{eff}}$ over which the magnetic helicity varies (if evaluated over different volumes), so we expect $k_{\text{eff}} \leq k_1$. Equation (4) becomes then

$$\mp d\langle \bar{\mathbf{B}}^2 \rangle / dt = \pm 2\eta k_1^2 \langle \bar{\mathbf{B}}^2 \rangle - 2\eta k_{AB}^{-1} \langle \mathbf{j} \cdot \mathbf{b} \rangle \pm 2\eta_t k_{\text{eff}}^2 \langle \bar{\mathbf{B}}^2 \rangle, \quad (7)$$

so the solution for the mean magnetic field is (assuming again $\langle \mathbf{j} \cdot \mathbf{b} \rangle \approx \pm k_f B_{\text{eq}}^2 / \mu_0$) given by

$$\frac{\langle \bar{\mathbf{B}}^2 \rangle}{B_{\text{eq}}^2} \approx \frac{\eta k_f k_{AB}}{\eta k_1^2 + \eta_t k_{\text{eff}}^2} \left\{ 1 - \exp \left[-2 \left(\eta k_1^2 + \eta_t k_{\text{eff}}^2 \right) (t - t_{\text{sat}}) \right] \right\}. \quad (8)$$

Thus, the time dependence is no longer resistively dominated, because the microscopic diffusivity is now supplemented by an additional turbulent diffusivity. Unfortunately, however, the amplitude of the final field decreases in such a way that the initial linear growth is unchanged. This is simply because of the fact that the flux term, as modelled here, does not act as an effective driver, which is what the $\langle \mathbf{j} \cdot \mathbf{b} \rangle$ -term did. This is also clearly seen in a simulation where we have included an equator by modulating the forcing function such that the kinetic helicity varied sinusoidally in the z -direction within the domain; see Figure 4.

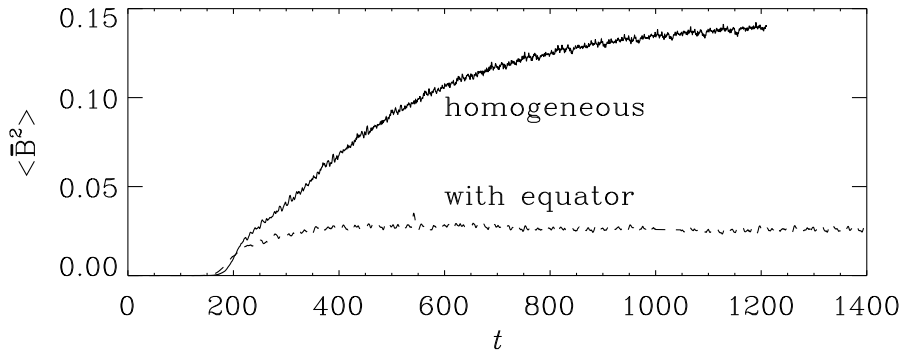


Figure 4. Evolution of the magnetic energy for a run with homogeneous forcing function (solid line) and a forcing function whose helicity varies sinusoidally throughout the domain (dotted line) simulating the effects of an equator.

5. Conclusions

The present work has shown that for helical velocity fields a large scale magnetic field is generated. There are strong parallels with the fields re-

sulting from mean-field α^2 -dynamos (see B2000 for details). One aspect that has now begun to receive major attention is related to magnetic helicity conservation, which prevents rapid growth of magnetic helicity and hence helical large scale magnetic fields. Shear, which corresponds to differential rotation in a rotating system, relaxes this constraint only partially in that it lowers the fraction of the field that contributes to magnetic helicity. On the other hand, by allowing magnetic flux to escape through the boundaries, or allowing for mixing of magnetic helicity of opposite sign at the equator, the helicity constraint is modified such that the time scale is no longer resistively dominated. The problem however is that various attempts to model this effect result in significantly lower equilibrium amplitudes of the magnetic field. Part of the problem is that the loss of magnetic helicity implies at the same time a loss of magnetic energy. It would therefore be advantageous for the dynamo to lose preferentially small scale magnetic helicity and energy. This is something that the dynamo in the computer keep refusing to do. It may therefore be important to resort to more realistic simulations where the flows are driven naturally and not by some artificial stirring in space.

References

Berger, M., & Field, G. B. (1984) The topological properties of magnetic helicity. *J. Fluid Mech.* **147**, 133–148

Berger, M. A., & Ruzmaikin, A. (2000) Rate of helicity production by solar rotation. *J. Geophys. Res.* **105**, 10481–10490

Blackman, E. G., & Field, G. F. (2000) Constraints on the magnitude of α in dynamo theory. *Astrophys. J.* **534**, 984–988

Brandenburg, A. (2000) The inverse cascade and nonlinear alpha-effect in simulations of isotropic helical hydromagnetic turbulence, *Astrophys. J.*, astro-ph/0006186 (B2000)

Brandenburg, A., & Subramanian, K. (2000) Large scale dynamos with ambipolar diffusion nonlinearity. *Astron. Astrophys.* **361**, L33–L36

Brandenburg, A., Bigazzi, A., & Subramanian, K. (2000) The helicity constraint in turbulent dynamos with shear, *Mon. Not. Roy. Astron. Soc.*, astro-ph/0011081

Frisch, U., Pouquet, A., Léorat, J., Mazure, A. (1975) Possibility of an inverse cascade of magnetic helicity in hydrodynamic turbulence. *J. Fluid Mech.* **68**, 769–778

Kleeorin, N. I., Moss, D., Rogachevskii, I., & Sokoloff, D. (2000) Helicity balance and steady-state strength of the dynamo generated galactic magnetic field. *Astron. Astrophys.* **361**, L5–L8

Krause, F., & Rädler, K.-H. (1980) *Mean-Field Magnetohydrodynamics and Dynamo Theory*. Pergamon Press, Oxford

Moffatt, H. K. (1978) *Magnetic Field Generation in Electrically Conducting Fluids*. CUP, Cambridge

Pouquet, A., Frisch, U., & Léorat, J. (1976) Strong MHD helical turbulence and the nonlinear dynamo effect. *J. Fluid Mech.* **77**, 321–354

Steenbeck, M., Krause, F., & Rädler, K.-H. (1966) Berechnung der mittleren Lorentz-Feldstärke $\mathbf{v} \times \mathbf{B}$ für ein elektrisch leitendes Medium in turbulenter, durch Coriolis-Kräfte beeinflußter Bewegung. *Z. Naturforsch.* **21a**, 369–376 See also the translation in Roberts & Stix (1971) The turbulent dynamo, Tech. Note 60, NCAR, Boulder, Colorado